Electronic Structure Measurements of Oxidized Flavins and Flavin Complexes Using Stark-Effect Spectroscopy

Robert J. Stanley* and Haishan Jang

Department of Chemistry, Temple University, Philadelphia, PA 19122

Received: June 4, 1999; In Final Form: August 26, 1999

Stark-effect spectroscopy (electroabsorption) measurements were obtained for oxidized flavin adenine dinucleotide (FAD) and flavin mononucleotide (FMN) in frozen glycerol/H_2O glasses and N(3)-methyl-N(10)-isobutyl-7,8-dimethyl-isoalloxazine in frozen *n*-butanol glasses at fields of up to 5×10^5 V/cm. In all three flavins, the effect of the applied electric field on the low-energy transition ($S_0 \rightarrow S_1$, 450 nm band) is significantly smaller than on the higher energy transition ($S_0 \rightarrow S_2$, 370 nm band). The Stark spectra indicate that the magnitude of the permanent dipole moment in the S_1 state, $|\vec{\mu}_1|$ is only modestly different from the S_0 state, $|\vec{\mu}_0|$, and that there is little change in the mean polarizability for the $S_0 \rightarrow S_1$ transition. The electric field effect on the $S_0 \rightarrow S_2$ transition, however, shows that the magnitude of the dipole moment of the S_2 state is ∼60% larger than that of the S_1 state and that the change in the mean polarizability is much larger. Concentration studies indicate that the FAD dimer or larger FAD aggregates give a nonlinear enhancement of the electric field effect. The source of this enhancement is unknown but may have to do with the stacked isoalloxazine−adenine configuration extended over a dimer or larger cluster of FAD molecules.

Introduction

Flavins are extremely important biological cofactors due to their ability to transfer either one or two electrons in a wide variety of biological processes.[1−4] This is due to the fact that flavins are stable in oxidized, one-electron reduced (semiquinone) and two-electron reduced (hydroquinone) forms in proteins. While this redox chemistry normally takes place in the ground electronic state, it is becoming evident that the excited electronic states, accessible by absorption of a photon, play an important physiological role in the areas of DNA repair (photolyases)[5,6] and signal transduction (cryptochromes).[7,8] The DNA repair mechanism involves ultrafast electron transfer from a fully reduced FAD anion to a cyclobutylpyrimidine dimer DNA lesion.[9,10] DNA photolyase is unique among FAD-containing flavoproteins in that the adenine ring is in a stacked configuration relative to the isoalloxazine moiety.[11] The functional consequences of this stacked configuration are not known. In the case of the cryptochromes, it is not known whether photoexcitation of the reduced flavin leads to electron transfer or whether the cryptochrome protein undergoes a conformational change in response to absorption of a photon.[12] A detailed knowledge of the change in charge distribution upon photoexcitation will be valuable in understanding how these important DNA-modulating enzymes work.

The electronic structures of flavins have been studied extensively by many methods, including both absorption[13,14] and luminescence spectroscopy,[15−19] time-resolved fluorescence,[20−22] resonance Raman spectroscopy,[23,24] CARS,[25,26] CD spectroscopy,[27−29] photo-CIDNP,[30] NMR,[31−33] and linear dichroism.[34,35] It is, however, very difficult to obtain quantitative information regarding the electronic distribution of the excited states directly. In addition, there have been only a few theoretical studies of these photoreactive states.[18]

Stark spectroscopy[36] has been used to investigate the role of charge transfer and redistribution in a variety of proteins. The electronic changes accompanying light transduction by retinal have been studied by Mathies and Stryer.[37] The photosynthetic reaction center, a light-driven redox protein, has been studied extensively using electric field effects.[38,39] An attractive feature of Stark spectroscopy for the study of redox processes is its sensitivity to charge transfer states and changes in electronic structure caused by an optical transition.[40] To elucidate the role of the excited state in the areas of flavoprotein DNA repair and signal transduction, we have undertaken a systematic study of the electronic properties of several oxidized flavins in simple solvents using Stark spectroscopy.

Materials and Methods

FAD (sodium salt, 96%) and FMN (sodium salt, 99%) were obtained from Sigma and used without further purification. The N(3)-methyl-N(10)-isobutyldimethylisoalloxazine (N(3)-flavin) was a generous gift of Professor Vincent Rotello (Figure 1). Solutions of oxidized FAD and FMN were prepared in glycerol/H_2O (1:1). The pH of these solutions was 6.2 ± 0.3 over a range of 1 μM to 12 mM. N(3)-flavin was dissolved in *n*-butanol. Stock solutions were stored at −20 °C. Handling was done under yellow light as much as possible.

Stark Spectrometer. The Stark spectrometer is shown in Figure 2. The output of a 150 W Xe arc lamp (Oriel 66007) is focused into a $^1/_8$ m monochromator (CVI Laser CM110) operating with 2 nm band-pass. The monochromatic probe beam is collimated with a fused silica singlet plano-convex lens and passed through a Glan-Taylor polarizer (Karl Lambrecht) to obtain horizontally polarized light. This light passes through the sample held in a cryostat at 85 K (see below). After passing through the sample, the probe light is focused onto a UV-enhanced Si photodiode operating in photovoltaic mode (UDT 455-UV/LN). The photocurrent is amplified by a factor of 10^6−10^7 in a current−voltage amplifier (Keithley 427).

* Corresponding author. E-mail: rstanley@nimbus.temple.edu.

10.1021/jp991811w CCC: $18.00
Published on Web 10/22/1999

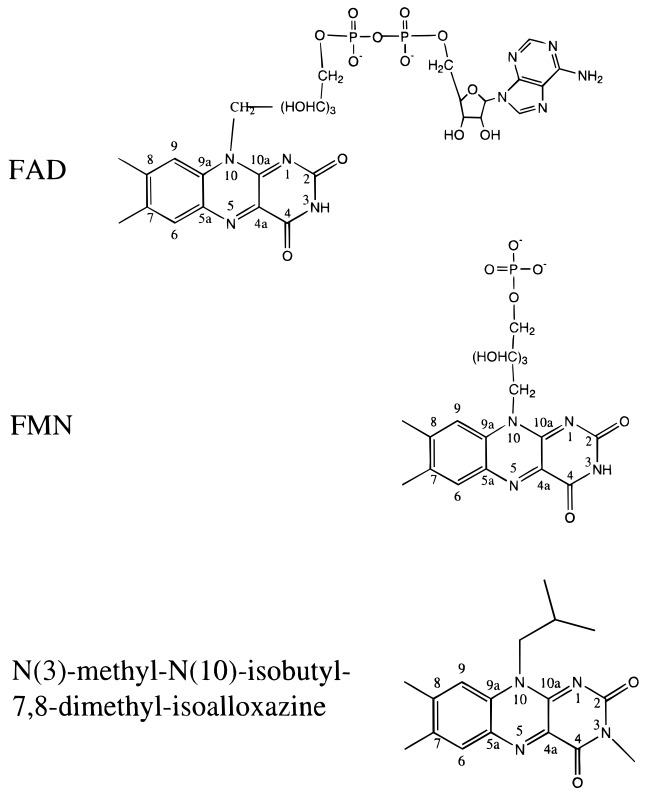

Figure 1. Flavins used in this study. FAD and FMN, are dissolved in glycerol/H_2O (1:1). N(3)-methyl-N(10)-isobutyl-7,8-dimethylisoalloxazine (hereafter referred to as N(3)-flavin) is dissolved in neat *n*-butanol.

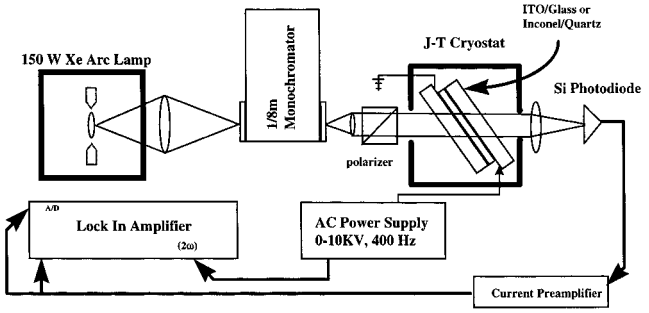

Figure 2. The Stark spectrometer.

The sample cuvette consists of two pieces of thin float glass or quartz substrate (~1.5 cm × 1 cm × 0.5−1 mm thick) each coated on one side by a transparent conductive layer of indium tin oxide (Delta Technologies) or inconel, OD 0.3−0.4 (Esco products), respectively. The conductive slides are separated by two ~50 μm thick strips (~0.2 cm × 1.0 cm) of either a epoxy-impregnated Mylar film (Ablestik 539IA) or an adhesive Mylar tape (Furon), leaving a gap between the slides for filling the cuvette. The epoxy-laden film/sample cuvette is thermoset using a hot plate at 150 °C for 5−7 min. The sample thickness was determined using a micrometer having 1 μm resolution. Three such determinations were averaged for each cuvette. The cuvettes are filled (~10 μL) with a syringe. For glycerol/H_2O samples it was necessary to pull the liquid through the cuvette using aspiration.

The cuvette was mounted onto the coldfinger of a unique cryostat (MMR Technologies). The cryostat uses a Joule−Thompson expansion of high purity gas through fine glass capillaries and is virtually vibration free. The temperature is monitored by a silicon diode at the tip of the coldfinger. The output of the diode is used to regulate the temperature to within ±0.1 K. Electric connections were made to the sample using fine insulated maganin wire soldered to molex-type connectors. Using 1800 psi of N_2 it is possible to achieve ≥80 K with about 250 mW of cooling. Because of the low heat capacity of N_2, initial cooling (at ambient pressure) was accomplished using high purity CH_4 at 1800 psi. Upon application of CH_4 the temperature dropped to <200 K in a matter of minutes. At this point, the cryostat vacuum chamber was evacuated and N_2 gas was used to achieve a working temperature of 85 K. The samples were extremely stable and the optical path pristine. The excellent signal-to-noise we have achieved is in large part due to the inherent noise-free operation of the refrigerator and the ability to maintain this state indefinitely, allowing extensive signal averaging. Because of its small size, the cryostat could be mounted on a rotation stage and its angle of incidence was set to either $\chi = 90°$ or $\chi = 55°$ relative to the polarization of the probe light. The 55° sample rotation has to be corrected for the differing indices of refraction for the substrate and solvent in order to obtain the true angle relative to the applied field which is $\chi = 66°$.

We have also used a LN_2 immersion Dewar (Brozk design, Cal-Glass for Research) to check these results, as most low-temperature Stark experiments are done by immersion. $\chi = 90°$ was used for these measurements because the Dewar windows are curved, not flat. The results were the same as those obtained with the J−T cryostat, within the signal-to-noise. One difference between the two methods is that LN_2 immersion gave moderately higher applied fields, perhaps due to better thermal contact with the sample and a higher dielectric breakdown threshold. However, the better signal-to-noise provided by the higher applied fields is somewhat offset by the large amount of scattering due to snow formation inside the immersion Dewar.

An AC high voltage generator (Joe Rolfe Associates) was used to supply the external electric field. The supply was driven with $\omega \approx 400$ Hz sine wave synthesized in the digital lock-in amplifier (SR830). This lock-in was used to detect the electric field modulated photodiode signal, ΔI, at 2ω. The amplified photodiode signal was also digitized to 16 bit precision by an analog-to-digital converter in the lock-in amplifier. This allows the Stark signal to be ratioed to the transmittance of the sample and also reduces the effect of lamp intensity fluctuations. Data acquisition was performed using in-house written Labview software (National Instruments) running on a Pentium-based computer. The computer-controlled monochromator is stepped to the desired wavelength rather than scanned. The lock-in was allowed to settle for 5 times the time constant setting before taking a reading. This eliminates the need to correct for time constant and coupled band-pass effects. Stark spectra were acquired using a step size of 2 nm with a time constant of 300 ms. Four scans were averaged and several such scans might be obtained at different fields from an individual sample. Since each run was taken at a different applied field, it was necessary to normalize them by dividing by the square of the applied field. Spectra from several different samples were co-added, after correcting for the applied electric field squared, to obtain the data shown below.

The field-induced change in the extinction coefficient was obtained by correcting the raw data for concentration and path length:[37]

$$\Delta\epsilon = \frac{2\sqrt{2}\,\Delta I(\vec{F})}{2.303 c l I_0} \qquad (1)$$

where $\Delta I(\vec{F})$ is the field-induced change in the transmission

through the sample, I_0 is the transmission through the sample in the absence of the field, the $\sqrt{2}$ corrects for the rms output of the lock-in, and the factor of 2 corrects for the collection of the Stark signal at 2ω. The data are divided by concentration c and the path length l to give $\Delta\epsilon$, the field-induced change in the molar extinction coefficient.

To obtain the low-temperature absorption spectra a cuvette was filled with buffer and frozen to 85 K to obtain the reference transmission. A chopper was used to modulate the probe beam (New Focus 3501). The cryostat was brought up to room temperature, and the cuvette was washed with several aliquots of the flavin solution. The flavin-containing cuvette was then brought to 85 K and the transmission measured again, giving the absorption spectrum $A = \log(I_{ref}/I_{flavin})$. The optical density of the sample was ~0.2 OD in ~50 μm path length for a 4 mM solution. Four scans were performed to obtain an absorption spectrum. Other room-temperature spectra (at lower concentrations) were obtained with a HP 8452 UV/vis spectrometer. Fluorescence studies were performed on a Spex Fluorolog-2 using a 4 × 10 mm Suprasil cuvette and calcite polarizers set for magic-angle detection.

Data Analysis. The Liptay formalism[41] is used to analyze the Stark spectra.

$$\frac{\Delta\epsilon}{\nu} = (f\vec{F})^2\left\{A_\chi\frac{\epsilon(\nu)}{\nu} + \frac{B_\chi}{15hc}\frac{\mathrm{d}[\epsilon(\nu)/\nu]}{\mathrm{d}\nu} + \frac{C_\chi}{30h^2c^2}\frac{\mathrm{d}^2[\epsilon(\nu)/\nu]}{\mathrm{d}\nu^2}\right\} \quad (2)$$

where $\vec{F}$ is the magnitude of the applied electric field, f is a correction for the local field felt by the solute molecule, h is Planck's constant, c is the speed of light, and $\epsilon(\nu)/\nu$ is the energy-weighted absorption spectrum corrected for concentration and path length. For an isotropically oriented immobilized (frozen) sample, A_χ is usually negligible. The B_χ term is related to the difference polarizability, $\Delta\bar{\bar{\alpha}} = \bar{\bar{\alpha}}_e - \bar{\bar{\alpha}}_g$, between excited and ground states,

$$B_\chi \approx \frac{5}{2}Tr\Delta\bar{\bar{\alpha}} + (3\cos^2\chi - 1)\left(\frac{3}{2}\hat{m}\cdot\Delta\bar{\bar{\alpha}}\cdot\hat{m} - \frac{1}{2}Tr\Delta\bar{\bar{\alpha}}\right) \quad (3)$$

where $Tr\Delta\bar{\bar{\alpha}}$ is the change in the mean polarizability and $\hat{m}\cdot\Delta\bar{\bar{\alpha}}\cdot\hat{m}$ is a component of the difference polarizability tensor along the transition moment of the molecule. The C_χ term contains information about the difference dipole moment, $\Delta\vec{\mu} = \vec{\mu}_e - \vec{\mu}_g$:

$$C_\chi = |\Delta\vec{\mu}|^2\{5 + (3\cos^2\chi - 1)(3\cos^2\zeta_A - 1)\} \quad (4)$$

where $\hat{m}$ is the transition dipole moment unit vector and ζ_A is the angle between $\Delta\vec{\mu}$ and $\hat{m}$ (see Figure 3). These equations relate χ, the direction of the applied electric field relative to $\hat{e}$, the polarization vector of the probe light, to the molecular frame by taking into account the fixed relationship between $\hat{e}$ in the lab frame and the transition dipole moment, $\hat{m}$, in the molecular frame. If spectra are obtained at any two angles, χ_1 and χ_2, then both eqs 3 and 4 can be rearranged as two equations in two unknowns to obtain $|\Delta\vec{\mu}|$ and ζ_A, or $Tr\Delta\bar{\bar{\alpha}}$ and $\hat{m}\cdot\Delta\bar{\bar{\alpha}}\cdot\hat{m}$.

Results

Low-Temperature Absorption Spectra. The low-temperature absorption spectra for FAD (1 mM) and FMN (4 mM) in glycerol/H_2O (1:1) and N(3)-flavin (4 mM) in *n*-butanol are shown in Figure 4. It is well-known that the two $\pi \rightarrow \pi^*$ transitions centered at 450 nm (band I) and 370 nm (band II, 350 nm in *n*-butanol) have a different response to temperature and solvent.[13,14,18] At room temperature and in polar solvents, both transitions are rather broad and featureless (data not shown). At cryogenic temperature, the 450 nm band is better resolved,

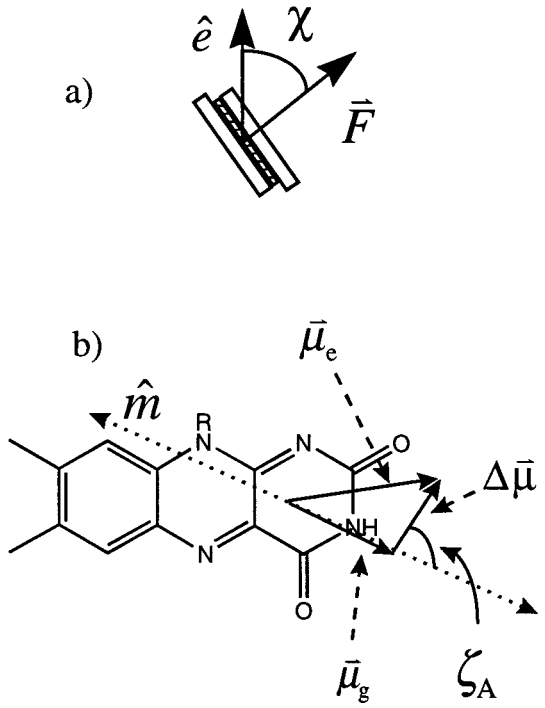

Figure 3. (a) The sample cuvette in the lab frame of reference. $\vec{F}$ is the applied electric field direction and $\hat{e}$ is the polarization direction of the probe light. χ is the angle between these two vectors. (b) The molecular frame of reference. The relationship between $\hat{m}$ and $\hat{e}$ connects the lab and molecular frames. ζ_A is the angle between $\hat{m}$ and $\Delta\vec{\mu}$. The 450 nm transition dipole moment, $\hat{m}$, is shown (···), which corresponds roughly with the direction of the ground-state dipole moment, $\vec{\mu}_g$ available from calculations.[48]

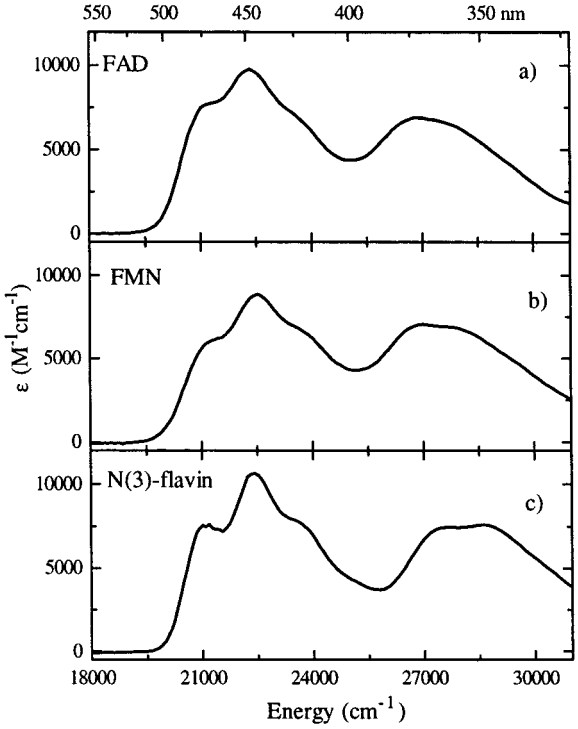

Figure 4. The low-temperature absorption spectra of FAD (1 mM), FMN (4 mM), and N(3)-flavin (4 mM), 85 K. The maximum of band I is at ~22 500 cm^{-1}, though the 0 → 0 transition is ~21 000 cm^{-1}. The position and maximum of band II is solvent dependent.

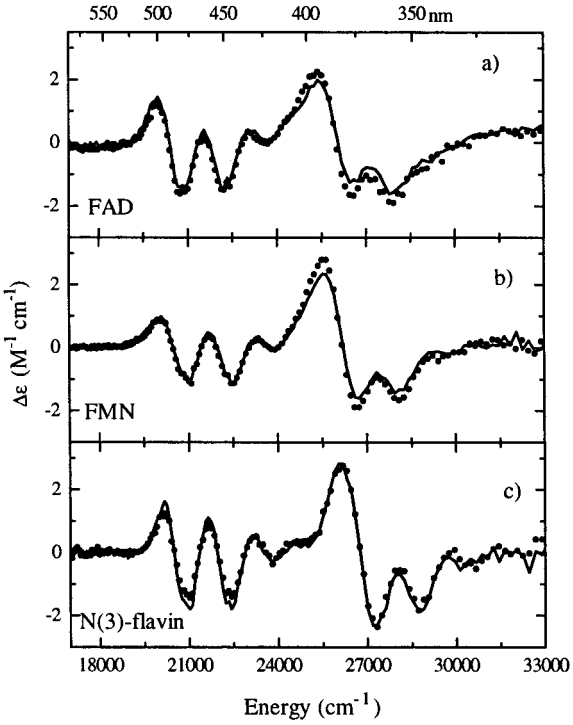

Figure 5. The Stark spectra for FAD, FMN, and N(3)-flavin at 4 mM, 85 K (dots, $\chi = 66°$; solid line, $\chi = 90°$). The spectra have been normalized to 1 MV/cm for comparison.

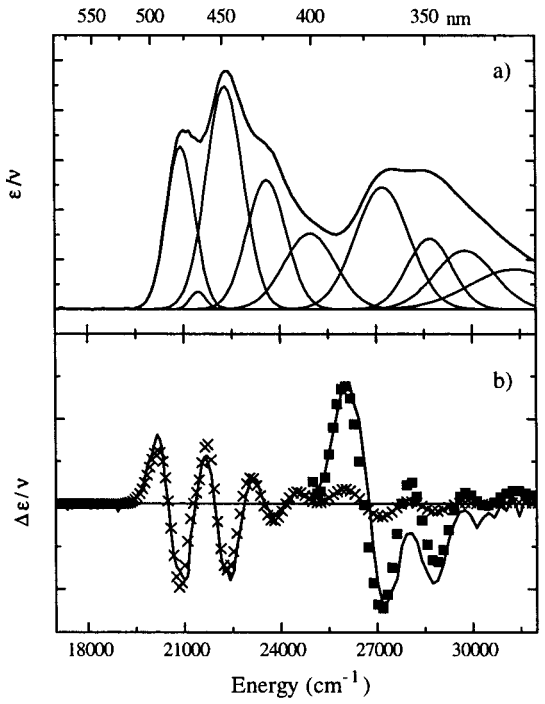

Figure 6. (a) The frequency-weighted absorption spectrum for N(3)-flavin in *n*-butanol at 85 K along with a Gaussian fit to the spectrum. (b) Stark spectrum for N(3)-flavin in *n*-butanol at 85 K, $\chi = 90°$ (—). Overlaying the Stark spectrum is the 2nd derivative of the (Gaussian-fit) absorption spectrum (×××) scaled to match band I. The second derivative was multiplied by a factor of 8 (■) in order to scale it to band II. There is still significant deviation from band II if only the second derivative is used.

presumably due to a decrease in inhomogeneous broadening.[17] In contrast, the 370 nm band is still rather broad, though better resolved in more nonpolar solvents. The peak extinction for flavins (band I) is about 10 000 M^{-1} cm^{-1}.

The spectrum of the N(3)-substituted flavin shows better resolution of the vibronic structure in both transitions. Band I shows virtually no shift in energy but narrows markedly. The increased resolution is similar to that observed in flavoproteins at room temperature[42] indicative of the hydrophobic nature of the flavin binding site. In contrast, band II shifts hypsochromically ~500 cm^{-1}. This band is known to be sensitive to both temperature and solvent polarity.[18,19] The blue shift is probably due to the loss of hydrogen bonding in aqueous solution that would lower the energy of the ground state more than the Franck−Condon excited state. An analysis of the Stark spectra (see below) demonstrates the importance of the polarizability in mediating this shift.

Low-temperature absorption spectra for FAD were obtained at 1, 4, and 12 mM in glycerol/H_2O glasses from 200 to 600 nm. The peak extinction coefficients were the same to within 10%, though the 12 mM spectrum falls off more slowly to the red edge of the 450 nm band (data not shown), perhaps a sign of hypochromism due to aggregation. Room-temperature measurements of the peak absorbance of the band I and band II were linear as a function of concentration over the range of 5 μM to 4 mM, though measurements on the 260 nm transition ($S_0 \rightarrow S_3$) showed a sublinear increase in absorption above 1 mM (data not shown).

Stark Spectra. In contrast to the absorption spectra, the Stark spectra for these flavins at 4 mM, $T = 85$ K, $\chi = 66°$, and $\chi = 90°$ are highly structured for both transitions (Figure 5). The largest change due to the applied field (4.3×10^5 V/cm) is $\Delta\epsilon \approx 2$ M^{-1} cm^{-1}, observed at ~26 000 cm^{-1}. The Stark signal is quadratic in the applied field within the experimental uncertainty (data not shown). Despite the small modulation, the signal-to-noise is high enough to allow features with $\Delta\epsilon/\epsilon_{max} < 10^{-5}$ to be measured. However, at optical densities below 0.05 (1 mM in 50 μm), the Stark signal becomes too noisy to provide high quality spectra. This lower limit is significant because the Stark spectra for flavins show a concentration dependence in the range available to us (see below).

In all three flavins, a comparison between the Stark and absorption spectra shows that the vibronic structure in the absorption spectrum can be well correlated with a series of minima in the Stark spectra. To bring out these correlations, most clearly we use the N(3)-flavin spectra as examples because the band separation is greater in *n*-butanol than in aqueous solvent. Figure 6a shows the absorption spectrum of N(3)-flavin plotted for comparison above the Stark spectrum at $\chi = 90°$ (6b). While the absorption spectra are of high quality, derivatives of the spectra enhance the noise. We have therefore fit the absorption spectra to a set of Gaussian functions (plotted in Figure 6a) which provide a smoothed set of derivatives. At present, we assign no physical meaning to this deconvolution, even though the Gaussian fit corresponds well with the vibronic structure in the low-temperature spectrum.

The contribution of $\Delta\mu$ to the Stark spectrum can be appreciated by plotting the numerical second derivative of the absorption spectrum (crosses) along with the Stark signal for the N(3)-flavin (solid line). To bring out the differences between the electric field response of band I and band II, the second derivative has been scaled to match the Stark spectrum around 22 000 cm^{-1}. While the 2nd derivative fits the 450 nm band well, it is clearly much too small to account for the 370 nm transition. This is not surprising since the two transitions might be expected to have significantly different electronic properties. This is implied by the differential sensitivity of the two bands to temperature, by their relative sensitivities to solvent polarity (Figure 4), and by their different transition dipoles.[34,35]

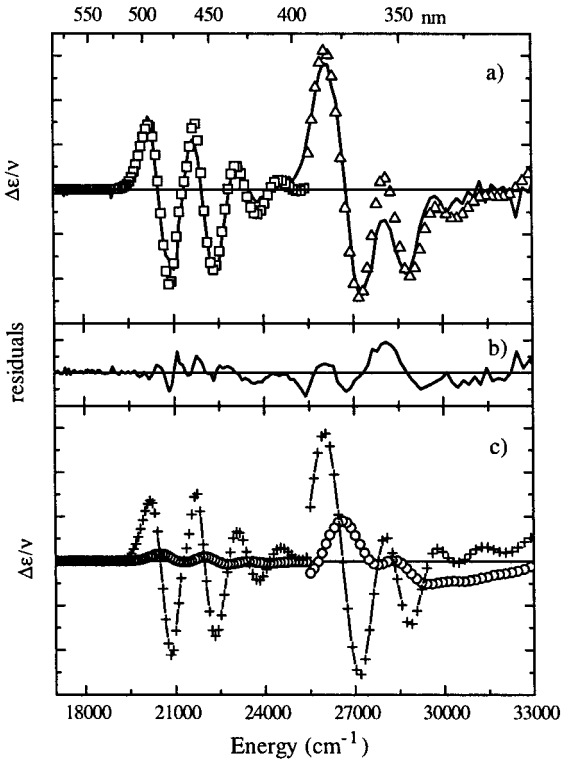

Figure 7. (a) The Stark spectrum and absorption spectrum are partitioned into two parts at about 25 000 cm^{-1}. The fits for these two partitions are shown (band I, squares; band II, triangles); (b) residuals of the fit, shown on the same scale as panel a; (c) the components of the fit: first derivative components (open circles); second derivative components (+++)

If the discrepancy between the two bands comes from a difference in $\Delta\vec{\mu}$ for each transition, then all that is necessary to fit these data is to scale the second derivative line shape by a weighting factor $(\Delta\vec{\mu}_{370}/\Delta\vec{\mu}_{450})^2$. This is shown in Figure 6b (squares), where we have made a separation of the two bands at ~26 000 cm^{-1} and $(\Delta\vec{\mu}_{370}/\Delta\vec{\mu}_{450})^2 = 8$. The 370 nm band is still not well fit by the second derivative. In particular, the Stark signal is shifted higher in energy relative to the second derivative, indicating that the first derivative component cannot be neglected. This is a signal that the two transitions have fundamentally different $\Delta\vec{\mu}$ and $\Delta\vec{\vec{\alpha}}$ values and that the Stark signal is very sensitive to these differences.

Fitting the Stark Spectra. The A_χ, B_χ, and C_χ parameters can be extracted from the data by fitting the frequency-weighted Stark spectrum, $\Delta\epsilon(\nu)/\nu$, to a linear combination of zeroth, first, and second derivatives of the absorption spectrum, $\epsilon(\nu)/\nu$ using eq 2. This is usually done by adjusting the A_χ, B_χ, and C_χ terms to give a best fit in a linear least-squares sense. When the absorption spectrum consists of overlapping transitions it is more difficult to extract these electronic structure parameters. The most straightforward procedure is to partition the spectrum into separate electronic transitions and obtain A_χ, B_χ, and C_χ for each transition individually.[43,44] The index separating the two partitions was varied until the error Σ(model Stark spectrum − Stark spectrum)^2 was minimized.[44] The model Stark spectrum was calculated from eq 2 for A^i,B^i,C^i, $i = 1-2$ for a given absorption spectrum fit. A linear least-squares fit of the derivatives of the absorption spectrum to the Stark spectrum is shown in Figure 7a and the residuals to the fit are shown in Figure 7b. This procedure produces a reasonable fit, matching the large feature at 27 500 cm^{-1} that was missed by a pure second derivative fit (cf. Figure 6b). The first and second derivative components of the fit are shown in Figure 7b, which shows that the 370 nm transition requires a much larger first derivative component than the 450 nm transition. However, the fit is relatively poor around 28 000 cm^{-1}.

To go further it is necessary to recognize that the quality of the fit depends on the fidelity of *both* the Stark and the absorption spectra. The absorption spectrum may contain artifacts because obtaining both the sample and reference transmission data necessitates removing, refilling, and replacing the cuvette, which can introduce error. Often the fragile glasses crack, creating scatter; this can be seen as sharp features superimposed on the overall absorption spectrum (cf. Figure 6a at ~21 000 cm^{-1}). The Stark spectrum does not suffer from this disadvantage, but the signals measured in this study are very small, in part because of the low output of our 150 W Xe arc lamp in the near-UV and the relatively high absorption of the cuvette glass and ITO coating.

To compensate for these difficulties, we have fit the absorption and Stark spectra simultaneously. The absorption spectrum of $j = 1 \rightarrow n$ Gaussian functions,

$$A(\nu) = \sum_j a_j \exp\left(\frac{-(\nu - \nu_j)^2}{2\Delta\nu_j^2}\right) + \text{baseline}$$

was allowed to vary in all parameters, the amplitude a_j, the Gaussian center ν_j, and the Gaussian width $\Delta\nu_j$. The absorption and Stark spectra were weighted equally. The minimizing parameter was taken to be the sum of the square of the residuals of the Stark and absorption spectrum fits. Fits were performed on at least three different samples for the Stark experiment, except for N(3)-flavin $\chi = 66°$ data of which only one data set was available. Several different deconvolutions for the absorption spectra were used. The number of Gaussians, n, for a deconvolution were also varied randomly. Additionally, A^i, B^i, and C^i initial values were varied. Approximately 10 such permutations were used to generate mean A^i, B^i, and C^i values so that standard deviations could be calculated.

The results of this procedure are summarized in Tables 1 and 2 and in Figure 8. The B and C terms for the three flavins are presented along with the values for $|\Delta\vec{\mu}|$, ζ_A, $Tr\Delta\vec{\vec{\alpha}}$, and $\hat{m}\cdot\Delta\vec{\vec{\alpha}}\cdot\hat{m}$ calculated as described following eqs 3 and 4. The large error for $\hat{m}\cdot\Delta\vec{\vec{\alpha}}\cdot\hat{m}$ in Table 2 appears to stem from the near zero B_χ^{450} values. Surprisingly, the tabulated values do not differ appreciably from those obtained without performing the simultaneous fit.

Concentration Dependence of the Stark Signal. Because of the low absorbance for 1 mM samples ($A \leq 0.05$), it has been difficult to obtain the concentration dependence of the Stark effect below 1 mM. This is important because flavins are known to aggregate even at low concentrations and it may be that the Stark spectra contain significant information on dimers or larger aggregates.[17,19] Gibson et al. used fluorescence quenching to study the dimerization of flavin mononucleotide (FMN) in aqueous solution.[45] They found an association constant K_D = 10 mM for 2FMN $\rightleftharpoons$ FMN_2 at room temperature. Using this value, a 4 mM solution of FMN should be ~25% dimers. If the extinction of the dimer is twice that of the monomer,[45] then half the absorption is due to the dimer at this concentration. At 1 mM flavin, the dimer concentration is ~8% at room temperature. The concentration of dimer is likely to be much higher at cryogenic temperatures. To address this issue, Stark spectra were obtained over a concentration range above 1 mM.

Stark spectra were obtained for FAD at 1, 4, and 12 mM concentrations (Figure 9a). The Stark signal is greatly enhanced

TABLE 1: *C* Terms, Difference Dipole Moments ($|\Delta\vec{\mu}|$), and ζ_A Values[a]

flavin	$C_{450}(66°)$	$C_{450}(90°)$	$C_{370}(66°)$	$C_{370}(90°)$	$\lvert\Delta\vec{\mu}_{450}\rvert$ (D/*f*)	ζ_A^{450} (deg)	$\lvert\Delta\vec{\mu}_{370}\rvert$ (D/*f*)	ζ_A^{370} (deg)
FAD	6.4 ± 0.6	6.5 ± 0.4	12.7 ± 1.2	11.8 ± 1.2	1.1 ± 0.2	52 ± 28	1.6 ± 0.3	42 ± 38
FMN	6.1 ± 0.3	6.5 ± 0.2	12.3 ± 0.7	12.0 ± 0.5	1.1 ± 0.1	71 ± 23	1.6 ± 0.1	50 ± 35
N(3)	5.1 ± 0.1	5.7 ± 0.5	13.3 ± 0.8	13.5 ± 1.0	0.9 ± 0.1	90 (−35)	1.6 ± 0.2	58 ± 30

[a] ζ_A must be $\leq 90°$.

TABLE 2: *B* Terms, Mean Polarizabilities ($Tr\Delta\vec{\vec{\alpha}}$), and Polarizability along the Transition Dipole Moment ($\hat{m}\cdot\Delta\vec{\vec{\alpha}}\cdot\hat{m}$)

flavin	$B_{450}(66°)$	$B_{450}(90°)$	$B_{370}(66°)$	$B_{370}(90°)$	$Tr\Delta\vec{\vec{\alpha}}_{450}$ (Å^3/*f*^{2})	$\hat{m}\cdot\Delta\vec{\vec{\alpha}}\cdot\hat{m}_{450}$ (Å^3/*f*^{2})	$Tr\Delta\vec{\vec{\alpha}}_{370}$ (Å^3/*f*^{2})	$\hat{m}\cdot\Delta\vec{\vec{\alpha}}\cdot\hat{m}_{370}$ (Å^3/*f*^{2})
FAD	0 ± 7	16 ± 8	394 ± 38	345 ± 37	-6 ± 9	-22 ± 24	177 ± 44	125 ± 113
FMN	-22 ± 6	-10 ± 7	267 ± 40	230 ± 36	-14 ± 8	-21 ± 20	121 ± 46	89 ± 116
N(3)	34 ± 6	34 ± 11	379 ± 16	363 ± 31	14 ± 9	5 ± 25	158 ± 25	75 ± 70

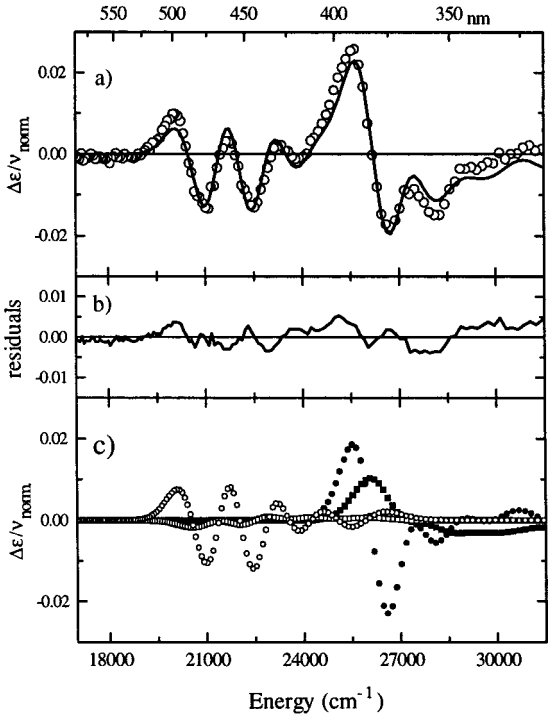

Figure 8. (a) The Stark spectrum for FMN at $\chi = 66°$ (open circles) and the fit (solid line) by simultaneously fitting both the Stark and absorption spectra (see text); (b) residuals; (c) components of the Stark fit. Band I: first derivative (open squares); second derivative (open circles). Band II: first derivative (solid squares); second derivative (solid circles).

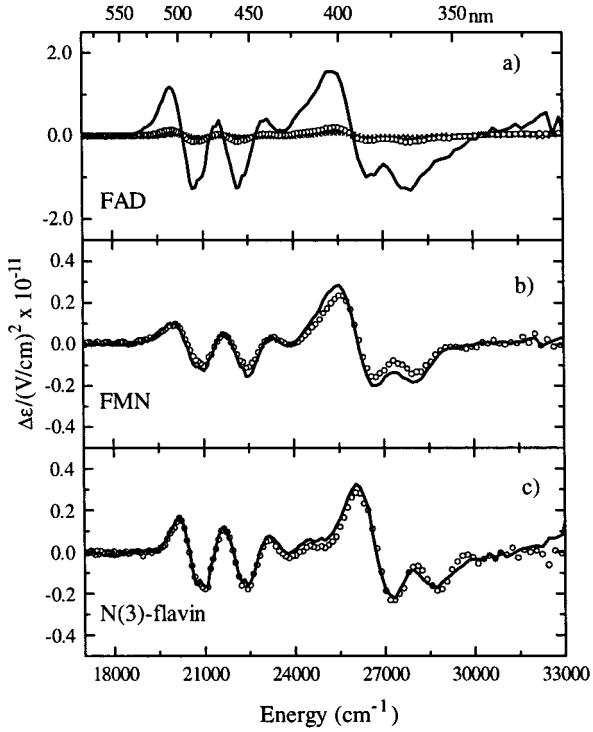

Figure 9. The concentration dependence of the Stark signal at $\chi = 90°$. All spectra have been normalized to 1 MV/cm for comparison: (a) FAD at 1 mM (×××), 4 mM (open circles), and 12 mM (—); (b) FMN at 4 mM (open circles) and 13 mM (—); (c) N(3)-flavin at 4 mM (open circles) and 13 mM (—).

at higher concentrations. The degrees of enhancement, from a linear least-squares fit of the 1 mM spectrum to the 4 and 12 mM spectra, are 2.4 and 22, respectively. This leads to a roughly exponential dependence of the Stark signal on concentration. Isosbestic behavior is observed, suggesting that a new species is forming quantitatively replacing the 1 mM species. A simple way to explain this discrepancy is that dimerization of the flavin changes the true concentration of flavin used to calculate $\Delta\epsilon$ (see eq 1). If we use 10 mM as the equilibrium constant for dimerization, then the corrected concentrations for the monomer would be $c' = 0.95$, 2.6, and 5.6 mM for the $c_0 = 1$, 4, and 12 mM data, respectively. Multiplying by the ratio c_0/c' (1.06, 1.54, and 2.14, respectively) should correct the data for this effect, assuming that the dimer does not contribute to the Stark signal and that that $K_D = 10$ mM. These correction factors predict the ratio of the Stark spectra should be 1:6:25, in the right range given the weak assumption that $K_D = 10$ mM at low temperature.

This correction, however, cannot explain the lack of a concentration effect for FMN and the N(3) flavin. In contrast to FAD, the effect of concentration on the Stark signal is very small for either species in the range of 4−13 mM (parts b and c of Figure 9; note the change in scale). At 4 mM, all three flavins give about the same Stark signal (see Figure 5). It is tempting to suggest that the FMN and N(3)-flavin spectra correspond to the monomer. However, given that the 1 mM FAD spectrum differs from the 4 mM FAD spectrum by a factor of 2.4, it may be that these molecules are completely converted to dimers at these concentrations. Another piece of evidence is that we have observed self-quenching of fluorescence emission in these compounds above 25 μM concentration (data not shown).

Discussion

Using Stark-effect spectroscopy, we have shown that the two lowest excited singlet states of oxidized flavins have quite different electronic properties. Both S_1 and S_2 states experience a modest change in dipole moment relative to the ground state. We obtained a $|\Delta\vec{\mu}_{450}|/f \approx 1$ D and $|\Delta\vec{\mu}_{370}|/f \approx 1.6$ D. The difference dipole moment for the 450 nm transition can be compared favorably with those obtained by microwave con-

ductivity[46] and solvatochromism measurements[47] where $|\Delta\vec{\mu}_{450}| \approx 1$ D. The ground-state dipole moment available from calculations is around 7 D.[48] Given that these transitions originate from the same ground state, the S_2 state is about 45% more dipolar than the S_1 state. More importantly, the 450 nm transition shows almost no change in the mean polarizability, *while the 370 nm band is 1−2 orders of magnitude larger in this respect.* It is this large change in polarizability that leads to the hypsochromic shift observed in the absorption spectrum as a function of solvent polarity.

Another important piece of information comes from the small effect of χ on the Stark signal. For $\chi = 66°$ and 90°, the $(3\cos^2\chi - 1)$ factor in eq 4 is -0.5 and -1, respectively. If ζ_A is any value significantly different from the magic angle (54.7°), the magnitude of the signal would be a fairly strong function of χ and we would have obtained very different C terms for $\chi = 66°$ versus $\chi = 90°$. This was not the case. For the 450 nm transition, the ground state permanent dipole moment is thought to be roughly collinear with the transition dipole moment.[48] If this is the case, then the magnitude of the S_1 permanent dipole moment can be estimated using the value of ${\zeta_A}^{450}$ from Table 1 and the law of cosines. For ${\zeta_A}^{450} \approx 65°$, obtained by averaging the FAD and FMN values, $|\vec{\mu}_{450}| \approx 7.5$ D/f.

The 370 nm transition shows a larger field effect, making the determination of ${\zeta_A}^{370}$ more precise. Using all three values gives ${\zeta_A}^{370} \approx 50°$. Proceeding as above, we arrive at $|\vec{\mu}_{370}| \approx 7.7$ D/f. The angle between the two transition dipole moments is about 20°, as measured by X-ray diffraction in flavodoxin single crystals.[34] This value can be used to determine the angle between the permanent dipoles for the 370 nm transition by using both the law of cosines and the law of sines. If we assume that $\vec{\mu}_{370}$ lies in the plane of the molecule then the angle between the S_0 and S_2 dipoles is roughly 11° and lies between the 370 and 450 nm transition dipoles.

What is also notable is that FMN and FAD have very similar Stark spectra at 4 mM. Given that FAD is likely in the stacked configuration at cryogenic temperature, it would not be surprising to see a relatively larger Stark signal if the adenine acts to decrease the "local" polarity of the solvent in the vicinity of the isoalloxazine chromophore. From NMR and CD experiments it is thought that the adenine ring is stacked on top of the xylene ring of the isoalloxazine moiety.[29−32] The lack of any large change in the Stark spectrum of FAD relative to FMN may be a clue that electronic redistribution due to the optical transitions is localized over the pyrazine−pyrimidine nuclei of the isoalloxazine. Circumstantial evidence for this conjecture comes from the absorption spectra of lumazines, which are just these nuclei without the xylene ring. These molecules have a $\pi \rightarrow \pi^*$ transition centered about ~410 nm at 77 K.[18] It will be interesting to measure the dipolar and polarizability properties for these molecules in order to compare them to flavins. These results suggest that these transitions can be used to probe protein-cofactor interactions with great sensitivity to the electrostatic details of the flavin binding site. The oxidized flavin can be used as an in situ probe to monitor changes in the charge distribution of the flavin binding site and, quite possibly, the electrostatic interactions between flavin and substrate. The ability to measure $|\Delta\vec{\mu}_{450}|$ and $|\Delta\vec{\mu}_{370}|$ simultaneously, along with their different transition dipole moment directions,[34,35] might allow for a "triangulation" of the perturbation. Along with the crystal structure it may be possible to pinpoint the interaction to a particular region of the protein binding site.

The issue of the aggregation of planar heterocyclic molecules has a long history. Other researchers have dealt with the problem of dimerization or polymerization of dyes in various solvents. Perhaps most relevant to this study is that of Zanker[49] who measured polymerization of acridine orange in ether−alcohol at low temperature. Mataga[50] examined the polymerization of flavin-like molecules in aqueous and organic solvents. These workers observed large shifts in the absorption specrtum as a function of concentration and temperature. However, the low-temperature absorption spectra of FAD shows only small changes as a function of concentration (<15% between 12 and 1 mM FAD, data not shown) and these changes are not monotonic nor show isosbestic behavior.

The spectral changes observed for most dyes are usually explained by exciton coupling between the transition dipole moments of the two monomers. There are configurations for dimers that lead to very little shift with very low intensity in one of the two exciton bands. If the transition dipoles of the monomers are orthogonal to each other then no exciton coupling is observed. However, it is hard to understand why this configuration would be preferred, especially since the appreciable *ground state* dipole moments, which lie in the plane of the isoalloxazine moiety, would tend to align in an antiparallel fashion. Since the transition dipole moments of either band I or II also lie in the isoalloxazine plane, there should be appreciable coupling and some evidence of dimerization in the absorption spectrum.

Hypochromism is another possible explanation for the lack of a spectral band shift. Hypochromism involves coupling the transition dipole from the first excited state of one of the monomers in a dimer with higher excited-state transition dipoles of the other monomer.[51] This leads to a change in the intensity of the excited molecule but does not invoke new bands or band shifts. At present, the low-temperature absorption data does not support this explanation but data at lower concentration is necessary in order to rule this out completely.

Despite the lack of spectral perturbations, we cannot assign the Stark spectra definitively to the monomer. However, given the lack of evidence for strong coupling between monomers and the lack of a concentration dependence for FMN and N(3)-flavin, we propose that the Stark spectra measured for these species represent the monomer spectra in the sense that dimerization does not influence the absorption spectrum measurably. Also, the difference dipole moment from these measurements agrees well with those available from experiments performed at lower concentration.

A solution to this quandary is to use flavoproteins, where high concentrations of flavins can be obtained without flavin−flavin dimerization. These studies will be crucial in order to assign the Stark spectra obtained in simple solvents to dimers or higher aggregates and are underway in our laboratories. Another possibility, given the high fluorescence quantum yield of oxidized flavins, is to measure the fluorescence Stark effect.[52,53] This technique is inherently more sensitive, so that measurements can be made at concentrations where dimerization is minimized. However, a detailed knowledge of the fluorescence quantum yields and other luminescence sources (e.g., phosphorescence, delayed fluorescence) are necessary in order to correctly interpret the results. Additionally, it is assumed that dimers or larger aggregates quench fluorescence quantitatively. While this has been observed for many molecules, aggregate emission has been observed for flavins in nonpolar solvents at low temperature.[17]

The nonlinear concentration dependence of the Stark signal for FAD suggests that the Stark signal may be due to flavin dimers and larger aggregates. Some observations about FAD

aggregation have appeared in the literature.[17,31,54] Sarma et al have suggested that a FAD dimer is formed by two stacked FAD monomers that have the adenine moieties opposed and the isoalloxazine units facing each other along the long axis.[54] Each nucleus of the isoalloxazine ring would be stacked over its like but the isoalloxazines rotated such that the carbonyl groups are staggered on the pyrimidine nucleus, leading to the least electrostatic repulsion. It is conceivable that this dimer might display very unusual properties relative to a dimer formed solely of isoalloxazine units. Indeed, excited state flavins are well-known to form charge transfer complexes with aromatic molecules like purines and pyrimidines, though usually this involves a triplet electronic state of the flavin.[55]

While the exact structure of FAD dimers is not known and may be fluxional, Rotello et al.[56,57] have synthesized model systems that hold the isoalloxazine ring in a particular configuration relative to a probe molecule having modifiable electronic properties. Flavins have large ground-state dipole moments so that dipole−dipole interactions lead to stacked configurations with a distance dependence of $1/r^3$. If dimer or aggregate formation is the cause of the nonlinear increase in the Stark signal for FAD, then these systems may have useful and interesting nonlinear optical properties. These scaffold-type systems should be ideal to test whether a dipole−dipole mechanism is important in flavin dimer formation and to determine how to exploit the inherent nonlinear optical properties of flavin arrays.

Flavoproteins, however, have very specific interactions with the flavin cofactor, often involving residues that are charged, polar, or polarizable. Additionally, the dielectric environment inside a protein is typically highly anisotropic. This can lead to large changes in $\Delta\epsilon$ through the local field correction, f, which is assumed to be relatively isotropic in simple solvents. If substantial ion−dipole or dipole−dipole interactions are in play inside the flavin binding pocket of the protein, there should be an enhanced Stark signal from these systems, whether they require light for function or not. Flavoproteins would show signature Stark spectra where it may be possible to relate these spectra to redox function and the dielectric nature of the cofactor binding site. Thus, this method will have general application for the study of structure/function relationships of these proteins.

In the case of DNA photolyase, the FAD cofactor is in a hairpin configuration, with the adenine stacked over the isoalloxazine ring.[11] This is the only flavoprotein known to have this structure. Given that this protein performs light-driven electron transfer, the interaction of the stacked configuration with the protein binding site and/or substrate (thymidine dimer) may have important functional consequences. This is particularly intriguing since we have observed a large change in the electronic properties of FAD upon aggregation. The protein or substrate may provide a similar enhancement of the electronic properties of FAD in order to modulate protein function.

Summary

We have measured the Stark spectra of FAD and FMN in glycerol/H_2O glasses and a nonpolar N(3)-methyl-N(10)-isobutyl-7,8-dimethylisoalloxazine in *n*-butanol glasses at 85 K. The electric field induced change in the extinction coefficient is small, suggesting that the difference dipole moments for the 370 and 450 nm transitions are also small, on the order of 1.1 D/f for the 450 nm transition and 1.6 D/f for the 370 nm transition. While the 450 nm transition is dominated by the difference dipole moment contribution, the 370 nm transition has a significant difference polarizability contribution that is much greater than that for the 450 nm transition. The FAD Stark signal demonstrates a concentration dependence that suggests that aggregation of FAD molecules produces a large change in the electronic properties relative to the monomer. Stark spectroscopy shows great promise for the study of flavoproteins in order to probe cofactor/residue or cofactor/substrate interactions at the electronic structure level. These studies are currently in progress in our laboratories.

Acknowledgment. We thank Professor Vince Rotello for the N(3)-flavin used in this study and for useful discussions. Discussions with Professors Marilyn Jorns, Linda Peteanu, Stefan Franzen, and Steve Boxer were also rewarding. We are grateful to the American Cancer Society (ACS IRG-204) for partial financial support of this work.

References and Notes

(1) Muller, F. Free Flavins: Syntheses, Chemical and Physical Properties. In *Chemistry and Biochemistry of Flavoenzymes*; Muller, F., Ed.; CRC Press: Boca Raton, 1991; Vol. I, pp 1−72.
(2) Stankovich, M. T. Redox Properties of Flavins and Flavoproteins. In *Chemistry and Biochemistry of Flavoenzymes*; Muller, F., Ed.; CRC Press: Boca Raton, 1991; Vol. I.
(3) Walsh, C. *Acc. Chem. Res.* **1980**, *13*, 148−155.
(4) Bruice, T. C. *Acc. Chem. Res.* **1980**, 256−262.
(5) Sancar, A. *Biochemistry* **1994**, *33*, 2−9.
(6) Heelis, P. F.; Okamura, T.; Sancar, A. *Biochemistry* **1990**, *29*, 5694−8.
(7) Hsu, D. S.; Zhao, X.; Zhao, S.; Kazantsev, A.; Wang, R.-P.; Todo, T.; Wei, Y.-F.; Sancar, A. *Biochemistry* **1996**, *35*, 13871−13877.
(8) Lin, C.; Robertson, D. E.; Ahmad, M.; Raibekas, A. A.; Jorns, M. S.; Dutton, P. L.; Cashmore, A. R. *Science* **1995**, *269*, 968−70.
(9) Kim, S. T.; Heelis, P. F.; Okamura, T.; Hirata, Y.; Mataga, N.; Sancar, A. *Biochemistry* **1991**, *30*, 11262−70.
(10) Okamura, T.; Sancar, A.; Heelis, P. F.; Begley, T. P.; Hirata, Y.; Mataga, N. *J. Am. Chem. Soc.* **1991**, *113*, 3143−5.
(11) Park, H.-W.; Kim, S.-T.; Sancar, A.; Deisenhofer, J. *Science* **1995**, *268*, 1866−72.
(12) Cashmore, A. R.; Jarillo, J. A.; Wu, Y.-J.; Liu, D. *Science* **1999**, *284*, 760−765.
(13) Harbury, H. A.; LaNoue, K. F.; Loach, P. A.; Amick, R. M. *Proc. Natl. Acad. Sci. U.S.A.* **1959**, *45*, 1708−1717.
(14) Müller, F.; Mayhew, S. G.; Massey, V. *Biochemsitry* **1973**, *12*, 46544662.
(15) Barrio, J. R.; Tolman, G. L.; Leonard, N. J.; Spencer, R. D.; Weber, G. *Proc. Natl. Acad. Sci. U.S.A.* **1973**, *70*, 941−943.
(16) Weber, G. *Biochem. J.* **1950**, *47*, 114−121.
(17) Eweg, J. K.; Müller, F.; Visser, A. J. W. G.; Visser, C.; Bebelaar, D.; Voorst, J. D. W. v. *Photochem. Photobiol.* **1979**, *30*, 463−471.
(18) Sun, M.; Moore, T. A.; Song, P.-S. *J. Am. Chem. Soc.* **1972**, *94*, 1730−1740.
(19) Song, P.-S.; Moore, T. A.; Kurtin, W. E. *Z. Naturforsch.* **1972**, *27b*, 1011−1015.
(20) Leenders, R.; Visser, A. J. W. G. *Proc. SPIE-Int. Soc. Opt. Eng.* **1992**, *1640*, 212−19.
(21) Leenders, R.; Kooijman, M.; Van Hoek, A.; Veeger, C.; Visser, A. J. W. G. *Eur. J. Biochem.* **1993**, *211*, 37−45.
(22) Leenders, R.; Roslund, J.; Visser, J. W. G. *J. Fluoresc.* **1995**, *5*, 349−53.
(23) Bowman, W. D.; Spiro, T. G. *Biochemistry* **1981**, *20*, 3313−18.
(24) Copeland, R. A.; Spiro, T. G. *J. Phys. Chem.* **1986**, *90*, 6648−54.
(25) Dutta, P. K.; Nestor, J.; Spiro, T. G. *Biochem. Biophys. Res. Commun.* **1978**, *83*, 209−16.
(26) Müller, F. The Flavin Redox-System and Its Biological Function. In *Topics in Current Chemistry*; Springer-Verlag: Berlin, 1983; Vol. 108, pp 71−107.
(27) Edmondson, D. E.; Tollin, G. *Biochemistry* **1971**, *10*, 113−124.
(28) Scola-Nagelschneider, G.; Hemmerich, P. *Z. Naturforsch.* **1972**, *27b*, 1044−1046.
(29) Miles, D. W.; Urry, D. W. *Biochemsitry* **1968**, *7*, 2791−2799.
(30) Stob, S.; Kemmink, J.; Kaptein, R. *J. Am. Chem. Soc.* **1989**, *111*, 7036−42.
(31) Kainosho, M.; Kyogoku, Y. *Biochemistry* **1972**, *11*, 741−752.
(32) Kotowycz, G.; Teng, N.; Klein, M. P.; Calvin, M. *J. Biol. Chem.* **1969**, *244*, 5656−5662.

(33) McCord, E. F.; Bucks, R. R.; Boxer, S. G. *Biochemistry* **1981**, *20*, 2880−8.
(34) Eaton, W. A.; Hofrichter, J.; Makinen, M. W.; Andersen, R. D.; Ludwig, M. L. *Biochemistry* **1975**, *14*, 2146−2151.
(35) Lennart, B.-Å. J.; Davidsson, Å.; Lindblom, G.; Naqvi, K. R. *Biochemistry* **1979**, *18*, 4249−4253.
(36) Hochstrasser, R. M. *Acc. Chem. Res.* **1973**, *6*, 263−269.
(37) Mathies, R.; Stryer, L. *Proc. Natl. Acad. Sci. U.S.A.* **1976**, *73*, 2169−2173.
(38) Lösche, M.; Feher, G.; Okamura, M. Y. *Proc. Natl. Acad. Sci. U.S.A.* **1987**, *84*, 7537.
(39) Boxer, S. G. *Adv. Photosynth.* **1996**, *3*, 177−189.
(40) Lockhart, D. J.; Boxer, S. G. *Biochemistry* **1987**, *26*, 664−8.
(41) Liptay, W. Dipole Moments and Polarizabilities of Molecules in Excited Electronic States. In *Excited States*; Lim, E. C., Ed.; Academic Press, Inc.: New York, 1974; Vol. 1, pp 129−229.
(42) Ghisla, S.; Massey, V.; Lhoste, J.-M.; Mayhew, S. G. *Biochemistry* **1974**, *13*, 589−597.
(43) Bublitz, G.; King, B. A.; Boxer, S. G. *J. Am. Chem. Soc.* **1998**, *120*, 9370−1.
(44) Premvardhan, L. L.; Peteanu, L. A. *J. Phys. Chem., submitted.*
(45) Gibson, Q. H.; Massey, V.; Atherton, N. M. *Biochem. J.* **1962**, *85*, 369−383.
(46) Shcherbatska, N. V.; Bastiaens, P. I. H.; Visser, A. J. W. G.; Jonker, S. A.; Warman, J. M.. In *Time-Resolved Laser Spectroscopy in Biochemistry III*; Lakowicz, J. R., Ed.; 1992; Vol. 1640, p 180.
(47) Shcherbatska, N. V.; van Hoek, A.; Visser, A. J. W. G.; Koziol, J. *J. Photochem. Photobiol. A: Chem.* **1994**, *78*, 241−246.
(48) Hall, L. N.; Orchard, B. J.; Tripathy, S. K. *Int. J. Quantum Chem.* **1987**, *31*, 217−242.
(49) Zanker, V. *Z. Physikal. Chem.* **1952**, *199*, 225.
(50) Mataga, N. *Bull. Chem. Soc. Jpn.* **1957**, *30*, 375−379.
(51) Cantor, C. R.; Schimmel, P. R. *Biophysical Chemistry*; W. H. Freeman and Company: New York, 1980; Vol. 2.
(52) Yeh, C.-Y.; Kamaya, H.; Ueda, I. *J. Lumin.* **1993**, *55*, 71−77.
(53) Lockhart, D. J.; Goldstein, R. F.; Boxer, S. G. *J. Chem. Phys.* **1988**, *89*, 1408−15.
(54) Sarma, R. H.; Dannies, P.; Kaplan, N. O. *Biochemistry* **1968**, *7*, 4359.
(55) Karen, A.; Ikeda, N.; Mataga, N.; Tanaka, F. *Photochem. Photobiol.* **1983**, *37*, 495−502.
(56) Breinlinger, E. C.; Rotello, V. M. *J. Am. Chem. Soc.* **1997**, *119*, 1165−1166.
(57) Deans, R.; Cook, G.; Rotello, V. M. *J. Org. Chem.* **1997**, *62*, 836−839.